Measurement of static constraints imposed by a human hand on a grasped object

Kazuya Matsuo, Kouji Murakami, Tsutomu Hasegawa, Kenji Tahara, and Ryo Kurazume

Abstract— **This paper proposes a method of directly measuring static constraints imposed by a human hand on a grasped object. Based on the analysis of the demonstration data of the human grasp, the static constraints are expressed as a combination of frictional force and normal force generated by the human hand. The static constraints are an important property to be mapped to robotic hands in the programming-by-demonstration. Measured static constraints are to be generated to robotic hands to establish the stable grasp. In the experiments, we have successfully measured the static constraints appeared in various different grasps used in the daily human life.**

I. Introduction

A multi-jointed multi-fingered robotic hand is a potentially dexterous hand like a human hand [1]. However, it is very difficult for us to manually and directly write a motion program of multiple fingers moving synchronously and cooperatively to execute a task. Programming-by-demonstration methods are often used in order to overcome this difficulty [2][3]. In programming-by-demonstration methods, a task program for the robotic hand is autonomously generated based on the motion data of actual tasks executed by a human. The tasks executed by a human are recognized from the motion data of his hand [4][5][6][7][8][9][10]: a continuous human motion is segmented, and symbolized according to the meaning of the particular motion in the context of the tasks. Each symbol represents a motion primitive, and a manipulation task by a human hand is represented as a sequence of symbols. The robotic hand will therefore be able to autonomously perform various tasks by executing a sequence of corresponding motion primitives if the symbols representing motion primitives are recognized.

Particular shapes of grasps by a human hand are usually used as keys to symbolize a human motion. When a man performs a manipulation task, he selects a hand shape properly depending on a shape of a grasped object and the purpose of the manipulation task. Appropriate hand shapes are different according to requirements for the manipulation task even if he grasps the same object. Cutkosky proposed a grasp taxonomy consisting of 16 hand shapes (Fig. 1) used by humans working with tools and metal parts [11]. Cutkosky classified the hand shapes based on shapes of the objects and purposes of the manufacturing task. Kamakura, an occupational therapist, proposed a grasp taxonomy consisting of 14 hand shapes (Fig. 2) used in daily life [12]. These classified hand shapes are called grasp types. The grasp types are usually used as the symbols representing motion primitives in programming-by-demonstration.

The static constraints imposed by the human hand are an important property to be mapped to the robotic hand in the programming-by-demonstration. The conventional approach so far has been based on the hand shape type observed typically in daily human life. Grasp types are based not on the static constraints but on the visual observation of hand shapes. Therefore, the robotic hand may not impose the appropriate static constraints on the grasped object when a shape-based grasp type is applied according to the observation of the human demonstration. In addition, a robotic hand can not reproduce grasp types if the configuration of the robotic hand is different from that of the human hand.

This paper shows that the static constraints of the grasp type are often different even if the same grasp type is performed by a human. In contrast to the conventional programming-by-demonstration, we propose a method of directly measuring the static constraints imposed by a human hand from the human demonstration data. We apply the static constraints as keys to segment human manipulation tasks for programming-by-demonstration. A robotic hand imposes appropriate static constraints on an object if measured static constraints are applied to the robotic hand.

The remainder of the present paper is organized as follows. Section Ⅱ describes the static constraints appeared in grasp. Formalization to obtain the static constraints is explained in Section Ⅲ. Section Ⅳ describes the devices to measure a motion of a human hand. Section Ⅴ describes the experiments for obtaining the static constraints from the hand shape type observed typically in the daily human life. The conclusions of the present study and the future works are presented in Section Ⅵ.

II. Static Constraints

Several works have been reported on the static constraints imposed by a robotic hand on a grasped object. Most of them focused on a finger force imposed on the grasped object at a contact point. The stability of the grasp is evaluated from the overall space of force and torque that can be applied by the grasp [13][14].

When a stable grasp is achieved, resistance force is generated according to external force applied to the grasped object. The resistance force is divided into the normal force and the frictional force, and each of them imposes the static constraint orthogonal to each other. We call DOF corresponding to the direction of static constraint imposed by the normal

K. Matsuo, K. Murakami, T. Hasegawa, K. Tahara, and R. Kurazume are with Graduate School of Information Science and Electrical Engineering, Kyushu University, 744 Motooka, Nishi-Ku, Fukuoka, 819-0395, JAPAN. matsuo@irvs.is.kyushu-u.ac.jp

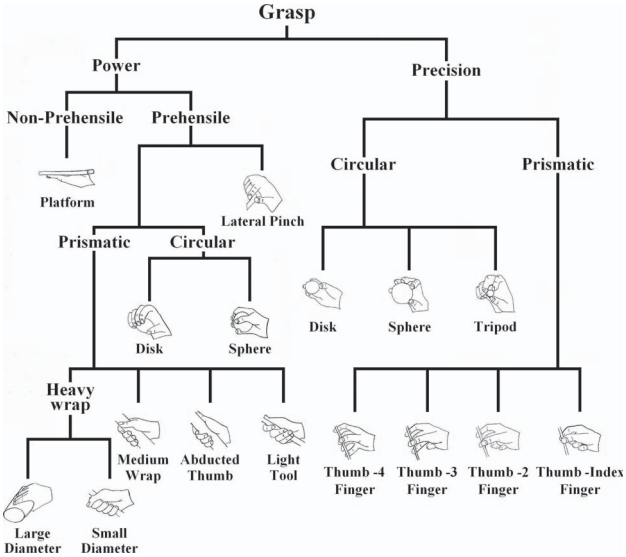

Fig. 1. Cutkosky's taxonomy of prehension [11].

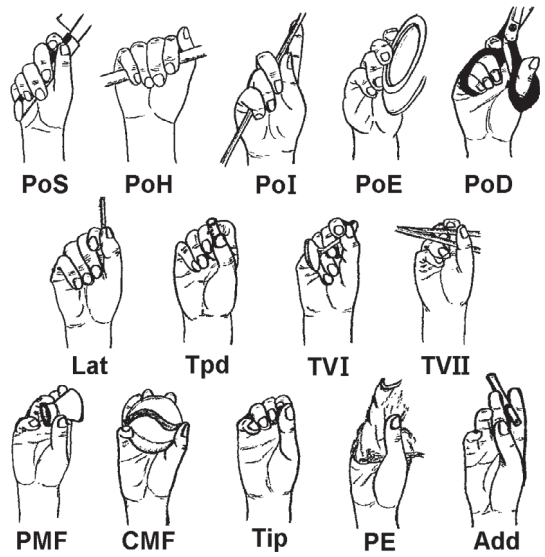

Fig. 2. Kamakura's taxonomy of prehension [12].

force *the normal DOF*. We call DOF corresponding to the direction of static constraint imposed by the frictional force *the frictional DOF*.

The difference of the static constraints of a normal DOF and a frictional DOF is shown as follows.

1) In the direction of the normal DOF, a human can apply force to an object up to the limitation of the stiffness of mechanisms of the human hand. However, the excessive inner force can damage the object.
2) In the direction of the frictional DOF, external force over the maximum static frictional force causes slipping. Therefore, excessive internal force is not applied to an object. However, a human may not apply enough force for a task to the object.

When a human grasps an object to perform a given task, he selects a combination of the normal DOFs and the frictional DOFs that are appropriate to the task. For example, we can see such assignment of the normal DOFs and the frictional DOFs in a writing task. A human grasps a pencil so that the direction of the shaft of the pencil coincides with the frictional DOF, thus avoiding excessive inner force to be imposed on the pencil. If he does not do so, the lead of the pencil is broken more easily. At the same time, he grasps the pencil in such a way that other DOFs are constrained as the normal DOFs, thus enabling the pencil fixed without undesirable move due to slipping. We can practically confirm that the normal DOFs and the frictional DOFs are assigned as mentioned above to establish the adequate static constraints in a human writing. Strategy to adjust the static constraints may be acquired through experience and learning of the worker. This strategy is expressed as a combination of the normal DOFs and the frictional DOFs in the selected grasp. Therefore, a robotic hand reproduce the knowledge and the strategy if the combination is mapped to the robotic hand in programming-by-demonstration. The previous work above mentioned does not distinguish the static constraints of a normal DOF and a frictional DOF. In contrast, we propose the static constraints as the combination of adequately selected normal DOFs and firictional DOFs.

We assume that a contact between the human hand and the grasped object is the point contact with friction. The resistance force is generated against external force at all the contact points. The resistance force at each contact point can be decomposed into normal force and frictional force. Six DOFs of the object, three translational DOFs and three rotational DOFs, are classified into two classes: normal DOFs and frictional DOFs.

We explain the normal DOFs and the frictional DOFs with a ball held by two fingers (Fig. 3). For the convenience of comprehension, we discuss a case of only the 3 translational DOFs. The normal force and the frictional force are generated at two contact points as Fig. 3 if external force is applied to the ball. In the vertical direction, the static constraint is imposed by the normal force. In contrast, in the horizontal direction and the depth direction, the static constraints are imposed by the frictional force. Therefore, the former are normal DOFs and the latter is frictional DOF.

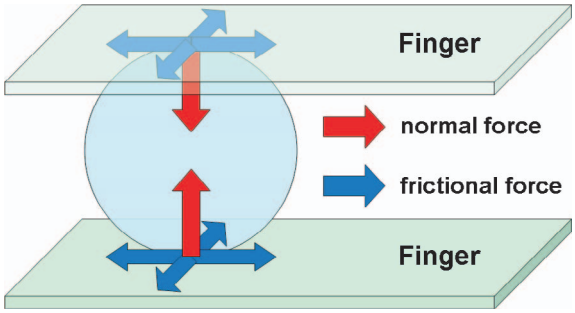

Fig. 3. Ball grasped by two fingers.

III. Formalization to Obtain Normal DOF

A hand performing a stable grasp can cancel an external force applied to the grasped object. This means that either the normal force or the frictional force acts along all the 6 DOFs of the object to maintain the stable grasp. Therefore, once the number of normal DOFs is identified, the number of frictional DOFs is obtained by subtraction as the rest of the 6 DOFs. So, we formulate a method for calculating the number of normal DOFs of a grasp in the translational DOFs and the rotational DOFs respectively.

A. Normal DOFs in the translational DOFs

Firstly, we construct a matrix: $\boldsymbol{W_f}$ is the matrix consisting of the unit normal vectors at all the contact points. The matrix is expressed as:

$$\boldsymbol{W_f} = \begin{pmatrix} \boldsymbol{f_1} & \boldsymbol{f_2} & \cdots & \boldsymbol{f_N} \end{pmatrix} \in \Re^{3\times N}, \tag{1}$$

where $\boldsymbol{f_i}$ is the unit normal vector at the i th contact point and N is the number of contact points (Fig. 4). $\boldsymbol{f_i}$ is expressed with respect to a coordinate system.

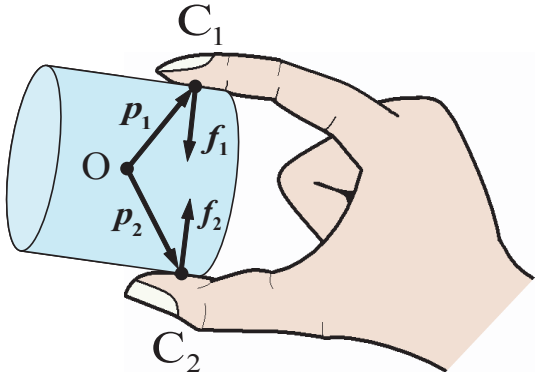

Fig. 4. Defined vectors to calculate the number of normal DOFs in the translational DOFs and the rotational DOFs: $\boldsymbol{f_i}$ is the unit normal vector at the i th contact point, $\boldsymbol{p_i}$ is the position vector of the i th contact point, and C_i is the i th contact point ($i = 1, 2$).

The number of normal DOFs in the translational DOFs is equal to $rank(\boldsymbol{W_f})$ because the normal force acts along the direction of the unit normal vector. Because the obtained motion data of the human hand contains an error, the number of normal DOFs in the translational 3 DOFs is calculated as follows (see Eq. 6 and Fig. 5):

$$\boldsymbol{W_f} = \boldsymbol{U\Sigma V^T}, \tag{2}$$

$$\boldsymbol{\Sigma} = diag(\sigma_1, \sigma_2, \sigma_3) \quad (\sigma_1 \geq \sigma_2 \geq \sigma_3 \geq 0), \tag{3}$$

$$\sigma'_1 = \frac{\sigma_1}{\sigma_1} = 1, \quad \sigma'_2 = \frac{\sigma_2}{\sigma_1}, \quad \sigma'_3 = \frac{\sigma_3}{\sigma_1}, \tag{4}$$

$$1 \geq \sigma'_2 \geq \sigma'_3 \geq 0, \tag{5}$$

$$\begin{gathered} if(\theta > \sigma'_2) \Rightarrow DOFs(\boldsymbol{W_f}) = 1 \\ else\ if(\theta > \sigma'_3) \Rightarrow DOFs(\boldsymbol{W_f}) = 2 \\ else\ DOFs(\boldsymbol{W_f}) = 3, \end{gathered} \tag{6}$$

where $DOFs(\boldsymbol{W_f})$ is the number of normal DOFs in the translational DOFs, σ_j ($j = 1, 2, 3$) are the singular values of $\boldsymbol{W_f}$, σ'_j are the singular values normalized by multiplying σ_1^{-1}, $\boldsymbol{U}$ are 3-by-3 orthogonal matrices, $\boldsymbol{V}$ are N-by-N orthogonal matrices, and θ is a threshold for eliminating the effect of measurement error.

We define a DOF along which both the normal force and the frictional force act as normal DOF, because the property of the static constraints along the DOF is more similar to that along normal DOF than that along frictional DOF.

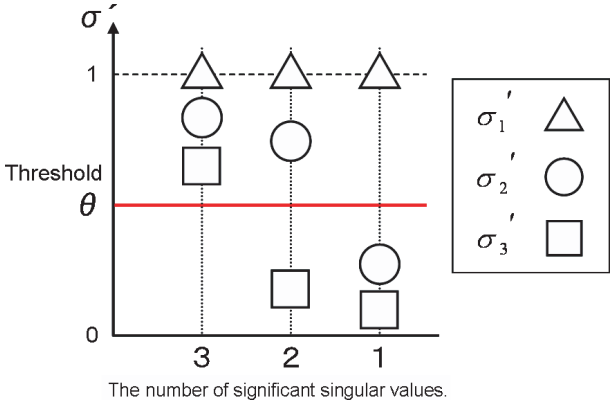

Fig. 5. Decision method for the number of significant singular values.

B. Normal DOFs in the rotational DOFs

The number of normal DOFs in the rotational 3 DOFs is calculated as follows:

$$\boldsymbol{t_i} = \boldsymbol{p_i} \times \boldsymbol{f_i} \ (1 \leq i \leq N), \tag{7}$$

$$\boldsymbol{W_t} = \begin{pmatrix} \boldsymbol{t_1} & \boldsymbol{t_2} & \cdots & \boldsymbol{t_N} \end{pmatrix} \in \Re^{3\times N}, \tag{8}$$

where $\boldsymbol{t_i}$ is the torque vector generated by $\boldsymbol{f_i}$, $\boldsymbol{p_i}$ is the position vector of the i th contact point, and $\boldsymbol{W_t}$ is the matrix consisting of all $\boldsymbol{t_i}$ (Fig. 4). $\boldsymbol{p_i}$ and $\boldsymbol{f_i}$ are expressed with respect to a coordinate system.

The number of normal DOFs in the rotational DOFs ($DOFs(\boldsymbol{W_t})$) is equal to $rank(\boldsymbol{W_t})$. $DOFs(\boldsymbol{W_t})$ is calculated in a similar method to the method of section III-A.

IV. Hand Model and Measurement Devices

A. Human hand model

We make a model of a human hand to calculate $\boldsymbol{W_f}$ and $\boldsymbol{W_t}$. The shapes of the links of the fingers are approximated to rectangular parallelepipeds. The shapes of the parts of the palm are approximated to prisms whose bases are surfaces of the palm. The lengths of the links, the width of the fingers and the size of the palm are decided based on the subject's right hand.

The hand model touches the grasped object on surfaces of the rectangular parallelepipeds and the bases of the prisms. We assume that a contact between the hand model and the grasped object is the point contact with friction. The shape of the subject's hand is computed from the hand model and the joint angles. Therefore, the unit normal vector ($\boldsymbol{f_i}$) at each

contact point is calculated once the joint angles of the human hand and the positions of all the contact points on surfaces of the hand model are measured. Then, $\boldsymbol{W_f}$ is obtained.

Moreover, $\boldsymbol{p_i}$ at each contact point is calculated once the center of mass of the grasped object are measured. Then, $\boldsymbol{W_t}$ is obtained.

B. Measurement Devices

We use two types of sensors to measure human hand motion, namely, a data glove and a tactile sensing glove designed by the authors. Joint-angle information and contact-position information are measured with the data glove and the tactile sensing glove respectively.

1) Joint-angle information: We use a Cyber Glove (CG1802-R: Immersion Corporation) as an input device for measuring the joint angles of a human hand. A photograph of the Cyber Glove is shown in Fig. 6. The specifications of the glove are shown in TABLE I. The Cyber Glove measures the angles of the eighteen joints of a human hand. In order to recognize grasp types, we use the angles of sixteen joints, excluding two joints of the wrist. The positions of the sixteen joints are shown in Fig. 7 and TABLE II. The proximal joint of the thumb has two DOFs, and the other fifteen joints have one DOF. The positions of the joint angles measured with the Cyber Glove correspond to the positions of the joints of the hand model shown in section IV-A. We assume that the angles of DIP (distal interpharangeal) joints are two thirds of the angles of PIP (proximal interpharangeal) joints of the fingers [15].

Fig. 6. Photograph of the Cyber Glove.

TABLE I

SPECIFICATIONS OF CYBER GLOVE

Number of Sensors	18
Sensor Resolution	0.5 degrees
Interface	RS-232
Maximum Data Rate	115.2 kbaud

2) Contact-position information: To measure the positions of contact points between a hand and a grasped object, we designed a tactile sensing glove. A total of 160 switches (EVQPLDA15 1.0: Matsushita Electric Industrial Corporation) are installed on the glove. A photograph of the glove and the placement of the 160 switches are shown in Fig. 8. The 160 switches are represented by circles in Fig. 8(b). The circles outside the contour of the hand indicate switches that are distributed on the sides of the fingers.

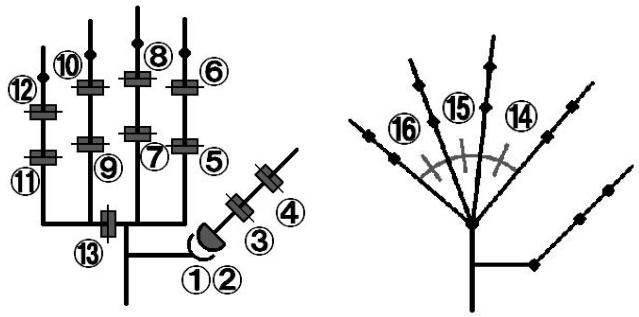

Fig. 7. Positions of the measured joints of the Cyber Glove.

TABLE II

THE MEASURED JOINTS OF THE CYBER GLOVE.

1	Thumb roll joint	9	Ring finger inner joint
2	Thumb-Index abduction	10	Ring finger middle joint
3	Thumb inner joint	11	Pinky finger inner joint
4	Thumb outer joint	12	Pinky finger middle joint
5	Index finger inner joint	13	Palm arch joint
6	Index finger middle joint	14	Middle-Index abduction
7	Middle finger inner joint	15	Ring-Middle abduction
8	Middle finger middle joint	16	Pinky-Ring abduction

Alternative switches, which output binary data of 'ON' or 'OFF', are used for the glove. The thickness of each switch is 0.8 mm, and the switches are squares having sides of 5 mm. The thickness of the contact mechanism of the switch is 0.4 mm, and the contact mechanism is circular, having a diameter of 3.2 mm. When a force of more than 1.0 [N] is exerted on the contact mechanism, the switch outputs the value of 'ON'. Contact information of the 160 positions on the hand are measured with the tactile sensing glove. The positions of the 160 switches on the hand model shown in section IV-A are known.

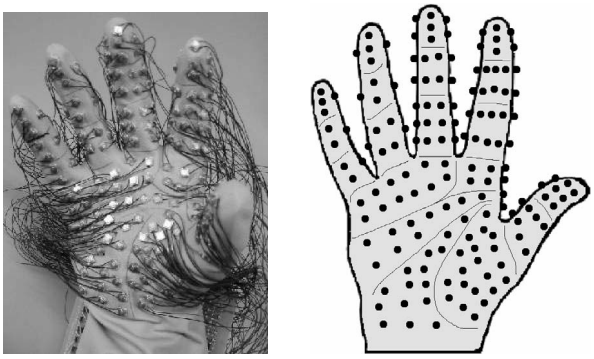

(a) (b)

Fig. 8. (a) Photograph of the tactile sensing glove with 160 switches. (b) Placement of the 160 switches.

V. EXPERIMENTS

We calculated the number of normal DOFs in the translational DOFs and the rotational DOFs at every grasp type defined by Cutkosky and by Kamakura. We measured the

joint-angle information and contact-position information at the 16 grasp types defined by Cutkosky and the 14 grasp types defined by Kamakura.

A subject wore the tactile sensing glove over the Cyber Glove while performing the 30 grasp types. He grasped objects commonly used in daily life (Fig. 9 and Fig. 10). He reproduced each grasp type 50 times in random order. A stable grasp was achieved in every grasp type. He was male of age 24 years. Although the thickness and the wiring of each glove may appear to be cumbersome, we confirmed through visual observation that the subject adequately performed the 30 grasp types (Fig. 11 and Fig. 12).

Fig. 9. Grasped objects used in the grasp types defined by Cutkosky.

Fig. 10. Grasped objects used in the grasp types defined by Kamakura.

We calculated the number of normal DOFs in the translational DOFs and the rotational DOFs at every grasp type by using the formalization and the hand model. The value of the threshold (θ) is 0.3. The counted number at every normal DOF is shown in TABLEs III and IV. A shaded cell indicates the biggest number at every grasp type.

These results are summarized as follows. The number of normal DOFs can be different even if the same grasp type is performed. For example, at the grasp type Precision Sphere in TABLE III, $DOFs(\boldsymbol{W}_f)$ is 2 when all contact points are on the circle of the sphere (Fig. 13-a), while $DOFs(\boldsymbol{W}_f)$ is 3 when the points are not on the circle (Fig. 13-b). At the grasp type PE in TABLE IV, $DOFs(\boldsymbol{W}_f)$ is 1 when

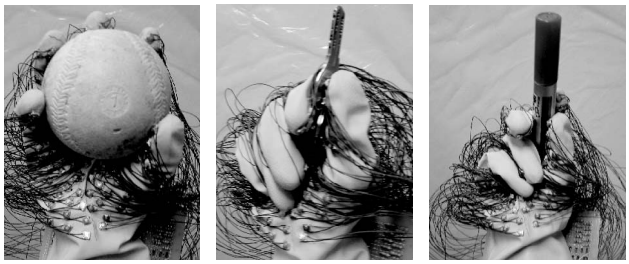

Power Sphere Lateral Pinch Tripod

Fig. 11. Photographs of several Cutkosky's grasp types.

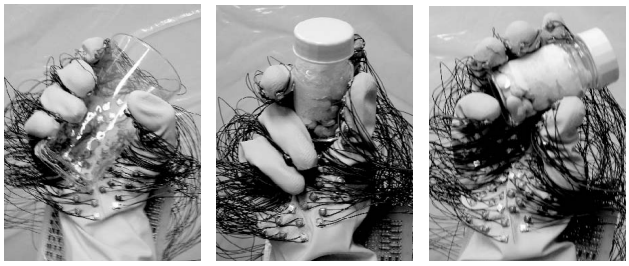

PoS Tpd PMF

Fig. 12. Photographs of several Kamakura's grasp types.

the grasped cloth is flat on a contact area (Fig. 14-a), while $DOFs(\boldsymbol{W}_f)$ is 2 or 3 when the cloth is not flat (Fig. 14-b). Static constraints can be different even if the same grasp type is performed. If we apply the conventional grasp types as keys to segment human manipulation tasks for programming-by-demonstration, the static constraints imposed by a human hand on a grasped object are not correctly reproduced by a robotic hand.

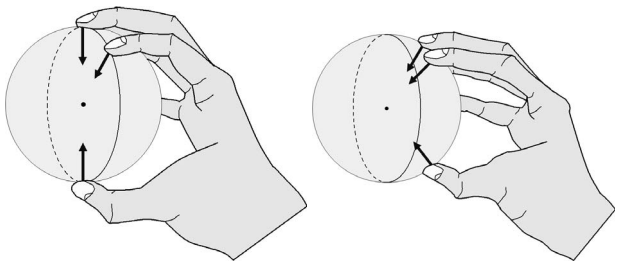

a: $DOFs(\boldsymbol{W}_f) = 2$ b: $DOFs(\boldsymbol{W}_f) = 3$

Fig. 13. Calculation of $DOFs(\boldsymbol{W}_f)$ for Precision Sphere.

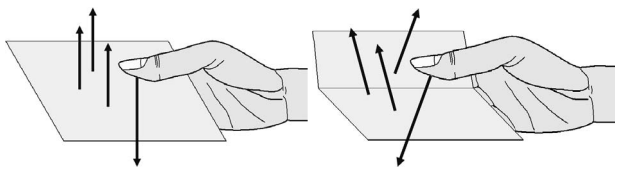

a: $DOFs(\boldsymbol{W}_f) = 1$ b: $DOFs(\boldsymbol{W}_f) = 2$ *or* 3

Fig. 14. Calculation of $DOFs(\boldsymbol{W}_f)$ for PE.

VI. Conclusions and Future Work

We have proposed a method of directly measuring the static constraints imposed by a human hand on a grasped

TABLE III

THE NUMBER OF NORMAL DOFS IN THE TRANSLATIONAL DOFS ($DOFs(\boldsymbol{W}_f)$) AND THE ROTATIONAL DOFS ($DOFs(\boldsymbol{W}_t)$) AT THE GRASP TYPES DEFINED BY CUTKOSKY.

Cutkosky's grasp types	$DOFs(\boldsymbol{W}_f)$			$DOFs(\boldsymbol{W}_t)$		
	3	2	1	3	2	1
Large Diameter	50	0	0	8	42	0
Small Diameter	50	0	0	50	0	0
Medium Wrap	38	12	0	33	11	6
Abducted Thumb	43	7	0	36	14	0
Light Tool	15	29	6	15	28	7
Power Sphere	50	0	0	24	26	0
Power Disk	50	0	0	50	0	0
Lateral Pinch	31	19	0	0	48	2
Platform	0	7	43	0	33	17
Precision Sphere	37	13	0	0	50	0
Precision Disk	29	21	0	0	50	0
Tripod	6	22	22	0	26	24
Thumb-4 Finger	50	0	0	0	50	0
Thumb-3 Finger	44	6	0	0	50	0
Thumb-2 Finger	50	0	0	7	43	0
Thumb-Index Finger	15	0	35	0	15	35

TABLE IV

THE NUMBER OF NORMAL DOFS IN THE TRANSLATIONAL DOFS ($DOFs(\boldsymbol{W}_f)$) AND THE ROTATIONAL DOFS ($DOFs(\boldsymbol{W}_t)$) AT THE GRASP TYPES DEFINED BY KAMAKURA.

Kamakura's grasp types	$DOFs(\boldsymbol{W}_f)$			$DOFs(\boldsymbol{W}_t)$		
	3	2	1	3	2	1
PoS	50	0	0	32	18	0
PoH	25	25	0	4	21	25
PoI	38	12	0	0	50	0
PoE	21	29	0	5	45	0
PoD	19	22	9	0	41	9
Lat	31	19	0	0	48	2
Tpd	44	6	0	0	50	0
TVI	22	28	0	0	47	3
TVII	12	38	0	10	39	1
PMF	0	48	2	2	46	2
CMF	50	0	0	24	26	0
Tip	6	22	22	0	26	24
PE	3	33	14	0	15	35
Add	0	0	50	0	0	50

object. The static constraints are expressed as a combination of the normal DOFs and the frictional DOFs. In the experiments, we successfully measured the static constraints at various grasp types used in daily human life. We confirmed that the static constraints were often different even if the same grasp type was performed. A manipulation task should be represented not as a sequence of conventional grasp types, but as a sequence of the static constraints. A robotic hand imposes appropriate static constraints on an object if measured static constraints are applied to the robotic hand.

Our future works are as follows. We will apply the static constraints as keys to segment human manipulation tasks for programming-by-demonstration. We will examine how the normal DOFs and the frictional DOFs are combined to establish adequate static constraints by a human hand in the manipulation tasks in the daily human life. We will map the measured static constraints to robotic hands in programming-by-demonstration.

REFERENCES

[1] A. Bicchi: "Hands for Dexterous Manipulation and Robust Grasping: A Difficult Road Toward Simplicity", IEEE Transactions on Robotics and Automation, Vol. 16, No. 6, pp. 652–662, 2000.

[2] K. Ikeuchi and T. Suehiro: "Toward an Assembly Plan from Observation Part I: Task Recognition With Polyhedral Objects", IEEE Transactions on Robotics and Automation, Vol. 10, No. 3, pp. 368–385, 1994.

[3] Y. Kuniyoshi, M. Inaba, and H. Inoue: "Learning by Watching: Extracting Reusable Task Knowledge from Visual Observation of Human Performance", IEEE Transactions on Robotics and Automation, Vol. 10, No. 6, pp. 799–822, 1994.

[4] J. Aleotti and S. Caselli: "Grasp Recognition in Virtual Reality for Robot Pregrasp Planning by Demonstration", Proceedings of the 2006 IEEE International Conference on Robotics and Automation, pp. 2801–2806, 2006.

[5] L. Y. Chang, N. S. Pollard, T. M. Mitchell, and E. P. Xing: "Feature selection for grasp recognition from optical markers", Proceedings of the 2007 IEEE/RSJ International Conference on Intelligent Robots and Systems, pp. 2944–2950, 2007.

[6] S. B. Kang and K. Ikeuchi: "Toward Automatic Robot Instruction from Perception - Mapping Human Grasps to Manipulator Grasps", IEEE Transactions on Robotics and Automation, Vol. 13, No. 1, pp. 81–95, 1997.

[7] K. Ogawara, J. Takamatsu, H. Kimura, and K. Ikeuchi: "Generation of a task model by integrating multiple observations of human demonstrations", Proceedings of the 2002 IEEE International Conference on Robotics and Automation, pp. 1545–1550, 2002.

[8] S. Ekvall and D. Kragic: "Grasp Recognition for Programming by Demonstration", Proceedings of the 2005 IEEE International Conference on Robotics and Automation, pp. 760–765, 2005.

[9] K. Bernardin, K. Ogawara, K. Ikeuchi, and R. Dillmann: "A Sensor Fusion Approach for Recognizing Continuous Human Grasping Sequences Using Hidden Markov Models", IEEE Transactions on Robotics, Vol. 21, No. 1, pp. 47–57, 2005.

[10] M. Kondo, J. Ueda, Y. Matsumoto, and T. Ogasawara: "Perception of Human Manipulation Based on Contact State Transition", Proceedings of the 2004 IEEE/RSJ International Conference on Intelligent Robots and Systems, pp. 100–105, 2004.

[11] M. R. Cutkosky: "On Grasp Choice, Grasp Models, and the Design of Hands for Manufacturing Tasks", IEEE Transactions on Robotics and Automation, Vol. 5, No. 3, pp. 269–279, 1989.

[12] N. Kamakura *et al.* : "Patterns of static prehension in normal hands", The American Journal of Occupational Therapy, Vol. 34, No. 7, pp. 437–445, 1980.

[13] J. K. Salisbury and B. Roth: "Kinematic and Force Analysis of Articulated Hands", ASME Journal of Mechanisms, Transmissions, and Automation in Design, Vol. 105, pp. 33–41, 1982.

[14] A. T. Miller and P. K. Allen: "Examples of 3D Grasp Quality Computations", Proceedings of the 1999 IEEE International Conference on Robotics and Automation, pp. 1240–1246, 1999.

[15] Y. Wu, J. Y. Lin, T. S. Huang: "Capturing Natural Hand Articulation", IEEE ICCV 2001, Vol. 1, pp. 426–432, 2001.